Annotating far-field diastolic electrograms delineates the midmyocardial isthmus in 3-dimensional ventricular tachycardia

Masato Okada, MD, Koji Tanaka, MD, Yusuke Ikada, BS, Nobuaki Tanaka, MD

From the Cardiovascular Center, Sakurabashi Watanabe Hospital, Osaka, Japan.

Introduction

Catheter ablation is an established treatment for scar-related ventricular tachycardia (VT). Automated annotation algorithms equipped with 3-dimensional (3D) mapping systems might be useful for revealing the tachycardia circuits of hemodynamically stable VTs without using electrophysiological techniques.[1,2] However, tiny fragmented long-duration potentials are often recorded in the critical isthmus,[3] and differentiating far- and near-field local electrograms (EGMs) is challenging. Additionally, it remains unknown how to approach EGMs with multiple components and how different the 3D mapping is according to the different annotation timings.

Recently, new discoveries have highlighted the limitations of representing human VT circuits on 2-dimensional (2D) surfaces. Many VT circuits are transmural, involving endocardial, midmyocardial, and epicardial pathways.[4,5] Here, we encountered a 3D-VT that exhibited multiple components within its isthmus EGMs. The isthmus image created using the manual annotation of the diastolic potentials was completely different from the one created using the automated algorithm.

KEY TEACHING POINTS

- Isthmus boundaries of macroreentrant ventricular tachycardias (VTs) have discontinuous electrograms, making it difficult to correctly differentiate near- and far-field electrograms.
- A block line created by the extended early-meets-late tool differs depending on which potential is being annotated.
- The correct annotation of near-field surface electrograms does not necessarily describe the midmyocardial isthmus in 3-dimensional VTs. Annotation of far-field electrograms in the diastolic phase sometimes clearly delineates the midmyocardium isthmus.

Case report

A 50-year-old man with a diastolic phase of hypertrophic cardiomyopathy was referred to our hospital for worsening heart failure and sustained VT. The QRS morphology exhibited a right bundle branch block configuration and right superior quadrant axis with a transition between V_3 and V_4 in the precordial leads, suggesting that the exit of the VT was in the inferior lateral region of the left ventricle (Supplemental Figure 1). After ruling out left ventricular thrombi and coronary artery disease using contrast-enhanced computed tomography, electrical cardioversion terminated the VT. However, the incessant occurrence of VT even after heart failure treatment and amiodarone administration (600 mg/day) led us to perform catheter ablation.

Catheter ablation was performed under general anesthesia using the CARTO 3 Version 7 system (Biosense Webster, Irvine, CA). A multielectrode catheter (PentaRay; Biosense Webster, Irvine, CA) was inserted into the left ventricle via a transseptal approach, and programmed ventricular stimulation repeatedly induced the clinical VT. Constant and progressive fusion during overdrive pacing supported the tachycardia with a macroreentrant mechanism (Supplemental Figure 1). Endocardial activation mapping of the left ventricle demonstrated a centrifugal spread with the earliest activation site located in the left ventricular posterior region. The total activation time within the left ventricular endocardium was 193 ms, which was shorter than the tachycardia cycle length (TCL) of 544 ms. There were no diastolic potentials recorded on the endocardial surface.

Then, epicardial mapping was performed during VT. Given the confined epicardial space, a linear decapolar mapping catheter (DECANAV; Biosense Webster, Irvine, CA) was used. The automated wavefront annotation algorithm did not clearly describe continuous circuit on epicardial surface with its total activation time of 460 ms, accounting for

KEYWORDS Annotation; Catheter ablation; Electrograms; Three-dimensional mapping; Ventricular tachycardia
(Heart Rhythm Case Reports 2023;9:893–897)

Address reprint requests and correspondence: Dr Masato Okada, Cardiovascular Center, Sakurabashi Watanabe Hospital, 2-4-32 Umeda, Kita-ku, Osaka, 530-0001, Japan. E-mail address: masato.okada1105@gmail.com.

https://doi.org/10.1016/j.hrcr.2023.09.013

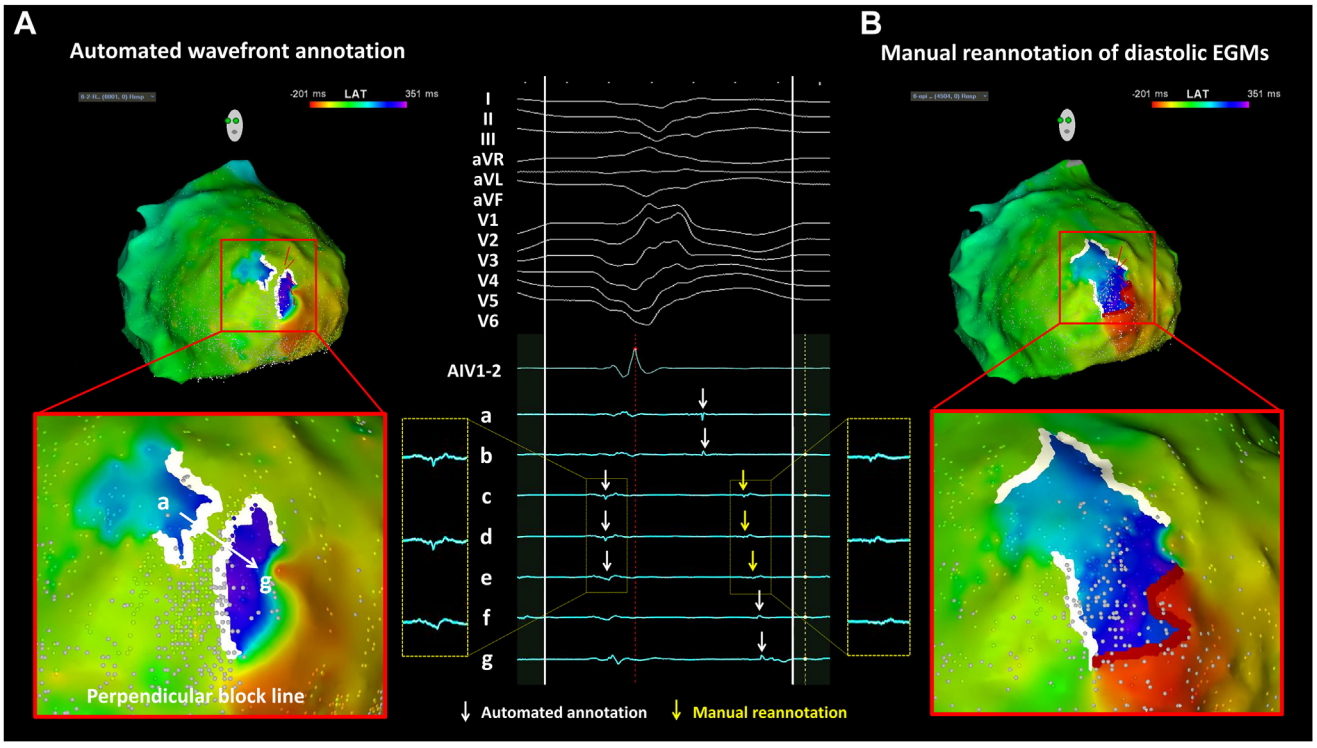

Figure 1 The electroanatomical maps recorded using the CARTO 3 system (Biosense Webster, Irvine, CA) are shown. The annotation window was set from 180 ms prior to the QRS onset to 370 ms after the QRS onset with the electrode catheter inserted into the distal anterior interventricular vein (AIV) as a reference, which is displayed as red in the ventricular tachycardia (VT) exit and blue and purple in the VT isthmus. Activation mapping created using an automated wavefront annotation (**A**) and manual reannotation of diastolic electrograms (EGMs) (**B**), respectively. The red line displays the early meets late, whereas the white line marks the local conduction block created by the extended early-meets-late algorithm with upper and lower thresholds of 90% and 30%, respectively. Local EGMs recorded from proximal to distal (from **a** to **g** in this figure) revealed widespread potentials through the isthmus (midpanel). In the middle of the isthmus (from **c** to **e**), the former and latter EGMs were estimated to be the high-frequency near-field surface EGMs and low-frequency far-field midmyocardial EGMs, respectively. The different timings of the EGM recordings contribute to the different block lines.

85% of the TCL of 544 ms. The extended early-meets-late (EEML) tool with its lower threshold of 30% displayed a noncontiguous isolated island with a U-shaped block line (Figure 1A). Across the block line, 2 discrete EGMs were observed: one during systole and the other during diastole. The former EGMs were estimated to be high-frequency near-field potentials in the systolic phase, whereas the latter ones were low-frequency far-field potentials in the diastolic phase. Manual reannotation of the latter EGMs made continuous isthmus activation with the EEML exhibiting lateral boundaries (Figure 1B). Because of the extensive low-voltage area on the epicardial surface (Figure 2A), the Ripple map did not clearly describe the diastolic activation (Supplemental Video 1). However, the Coherent activation map with conduction velocity vectors displayed a figure-of-eight circuit with its estimated common pathway in the slow or nonconducting zones (Figure 2B).

At the entrance of the lateral boundaries where all the vectors rejoined, ventricular overdrive pacing exhibited entrainment with concealed fusion, a stimulus-QRS interval (285 ms) equal to the EGM-QRS interval, and a postpacing interval (PPI) − TCL of 0 ms, indicating that the pacing site was in the central isthmus of the VT circuit (Figure 2A). We applied 30 W of radiofrequency energy with 10 g contact force at that site, which successfully terminated the VT within 1 second. The VT was no longer inducible and radiofrequency energy was additionally delivered until the ablation index reached 500 (using 30 W output for 30–40 seconds with an initial impedance of approximately 150 ohms and impedance decreases of 15–25 ohms). The procedure was completed without any complications after confirmation of the noninducibility of the clinical VT. The patient was discharged after continued administration of amiodarone (100 mg/day) and implantation of an intracardiac defibrillator. At 12 months postablation, no VT occurred until this report was written.

Discussion

Current mapping systems facilitate visualization of the complex VT circuit. However, the activation map is considerably influenced by how precisely each EGM is annotated, and various new tools and systems are being developed to improve this process. In the present case of a 3D-VT, 2 separate EGMs were recorded on the epicardial surface during the VT. The preceding one was an epicardial outer-loop near-field potential during the systolic phase and the other was a midmyocardial far-field potential during the diastolic phase.

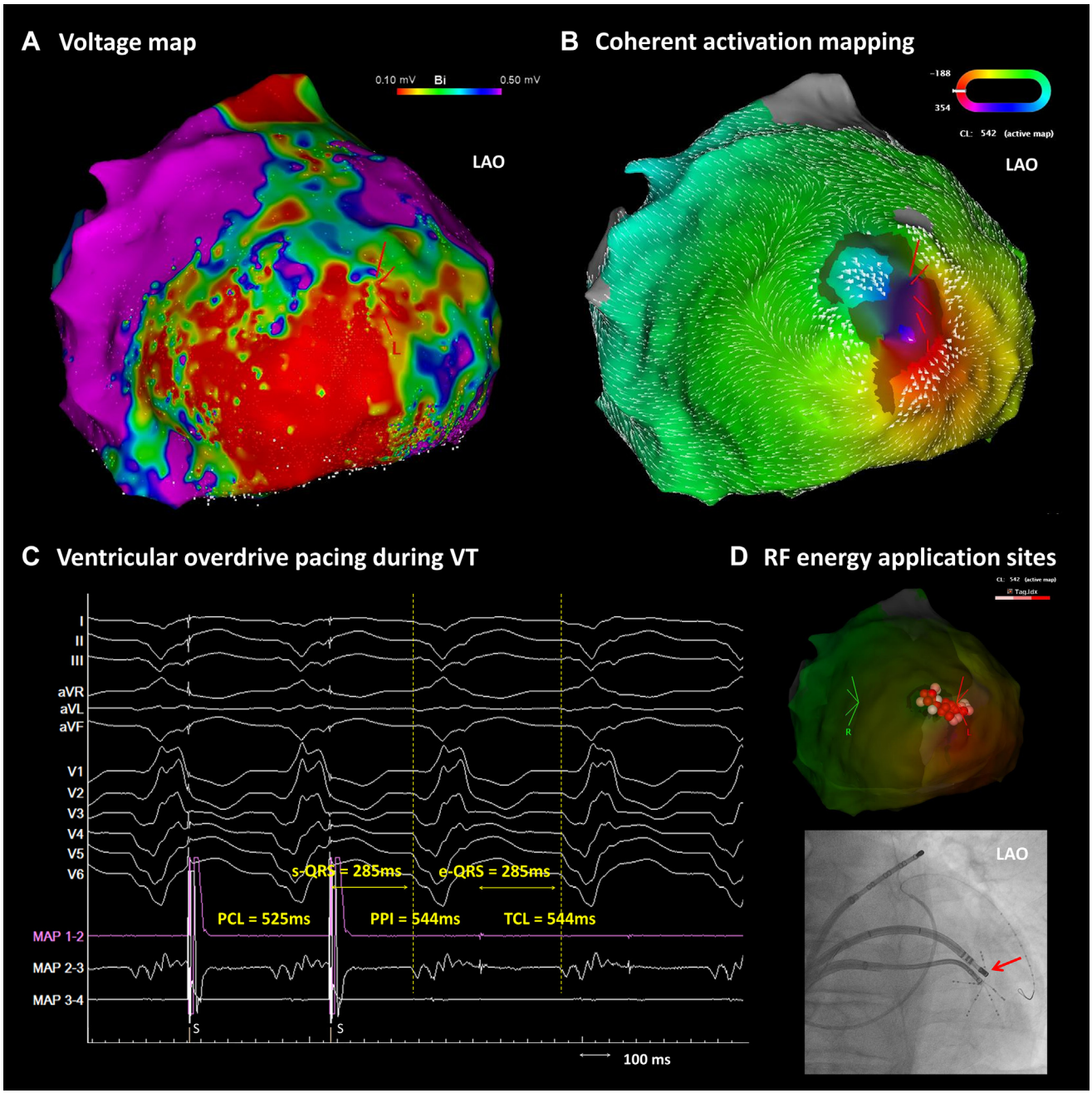

Figure 2 **A:** Voltage map during ventricular tachycardia (VT) with the low-voltage threshold set at 0.1–0.5 mV. **B:** Coherent activation mapping using the manual reannotation. **C:** Intracardiac electrograms during ventricular overdrive pacing at the successful radiofrequency energy application site. At that site, all the Coherent vectors rejoined and the tiny fragmented potentials during the diastolic phase were observed on the MAP catheter. Overdrive pacing from the distal MAP electrodes (MAP 1–2) revealed entrainment with concealed fusion, a stimulus-QRS (285 ms) equal to the electrogram-QRS, and a postpacing interval − tachycardia cycle length of 0 ms. The findings indicated that the pacing site was the "central isthmus" of the VT circuit. **D:** Radiofrequency energy application sites on the CARTO map (upper panel) and fluoroscopic image (lower panel). I, II, III, aVR, aVL, aVF, V1, V2, V3, V4, and V5 represent the surface electrocardiogram; and MAPs 1–2 to 3–4 represent the electrograms of the ablation catheter placed on the left ventricular epicardium. e-QRS = electrogram-QRS; LAO = left anterior oblique; PCL = pacing cycle length; PPI = postpacing interval; RF = radiofrequency; s-QRS = stimulus-QRS; TCL = tachycardia cycle length; VT = ventricular tachycardia.

The activation mapping and block line created by the EEML tool completely differed depending on the annotation timing.

Given that the CARTO 3 module sets the maximum negative dV/dt at the distal unipolar signal as the automated annotation point,[1,2] it may miss relevant low-amplitude delayed-activation EGMs and fail to display the isthmus activation patterns. In our case, however, the CARTO 3 dV/dt algorithm would correctly differentiate near- and far-field signals considering the frequency and nature of those EGMs. However, the "correct" annotation of near-field surface potentials did not clearly describe the isthmus, probably because the isthmus was located in the midmyocardium

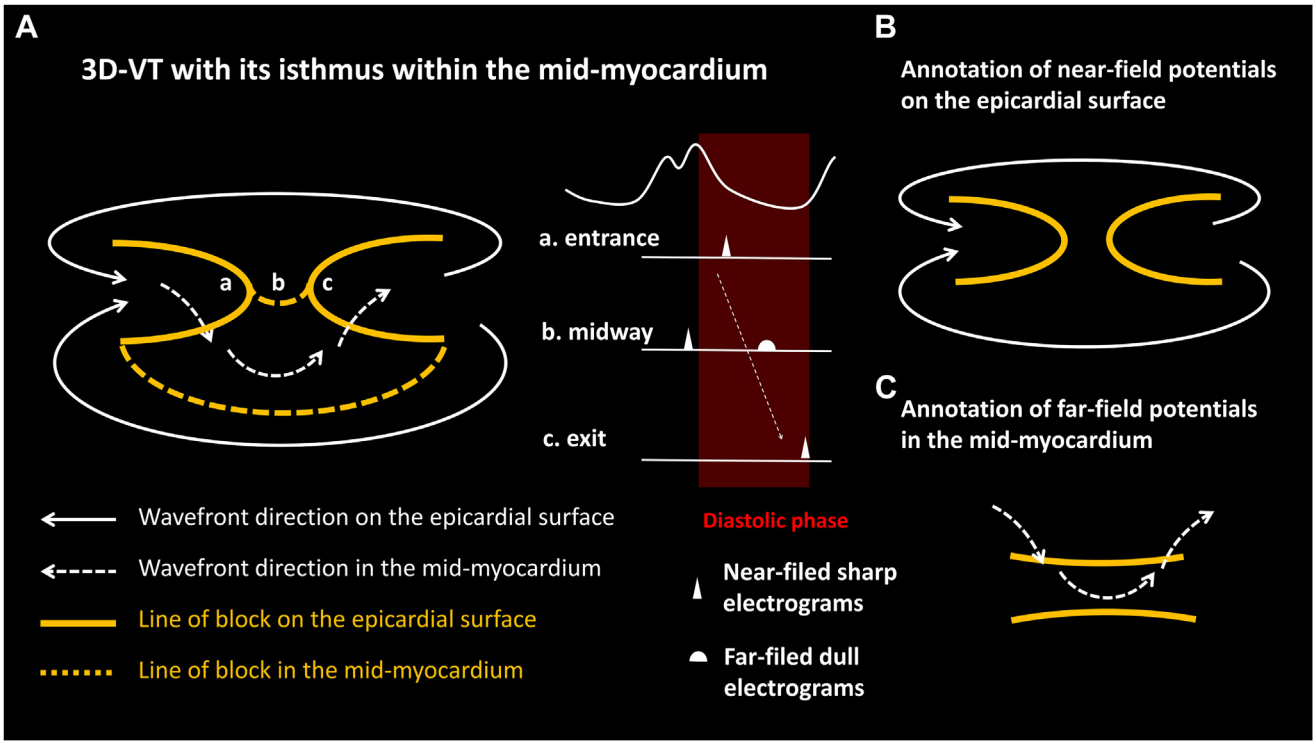

Figure 3 **A:** Schematic representation of our 3-dimensional ventricular tachycardia (VT) with its isthmus within the midmyocardium. The white solid and dotted arrows describe the wavefront direction on the epicardial surface and within the midmyocardium, respectively. The orange solid and dotted lines represent the block lines on the epicardial surface and in the subepicardium, respectively. The surface electrodes record both near-field sharp and far-field dull potentials on the midway of the midmyocardial isthmus. **B:** Annotation of near-field potentials creates a U-shaped block line on the epicardial surface. **C:** Annotation of far-field potentials during the diastolic phase creates lateral boundaries.

(Figure 3B). Conversely, when we focused on the diastolic potentials, which were the midmyocardial far-field potentials, the isthmus of the 3D-VT was clearly delineated between the white block line (Figure 3C). Although the EEML algorithm is somewhat arbitrary according to the threshold setting, the EEML algorithm provided objective evidence of the local conduction gaps and helped enhance their visualization.[6]

Certainly, the pursuit of the "correct" near-field recordings and annotation is important because the isthmus often has tiny, long-duration, and fragmented EGMs. Small electrodes and close interelectrode spacing have been shown to enhance the signal quality and enable differentiation between near- and far-field signals.[7] The use of the Ocatrary catheter (Biosense Webster, Irvine, CA) instead of the DECANAV might have created a different activation map in our case. Moreover, the bipolar EGMs are greatly influenced by the wavefront direction. Omnipolar EGMs would help resolve the directional dependency of the bipolar EGMs.[8] Furthermore, a new algorithm based on the peak frequency has recently become available to annotate near-field components. These technologies would delineate the VT circuit when the circuit is located on the 2D endocardial/epicardial surface.

However, the 2D perspectives may oversimplify human VT. In our case, annotation of the far-field signals uncovered the midmyocardial isthmus in the 3D-VT. Both systolic and diastolic EGMs are important constituents of macroreentrant VTs, and selecting one over the other may lead to erroneous descriptions of the complex electrophysiological phenomenon. Therefore, operators should recognize which potentials are prioritized in the constructed activation map: annotating systolic and diastolic potentials would mean prioritizing the outer-loop and isthmus potentials, respectively. When focusing on the isthmus in macroreentrant VTs, annotation of the last deflection under a fixed window from the QRS onset to the QRS onset[4] or setting the window of interest during the diastolic phase[9] are well-known methods. A 3D perspective of the VT circuit has enhanced the precision of the ablative therapy but revealed limitations in annotating near-field surface EGMs for circuit delineation.

Conclusion

In our 3D-VT case, the block line created by the EEML algorithm completely differed from that created by the automated algorithm and manual annotation of the diastolic potentials. Widespread abnormal potentials created by surface and midmyocardial EGMs may have contributed to this result. Correct near-field annotation of endocardial/epicardial surface EGMs may not necessarily allow us to describe the midmyocardial isthmus in human 3D-VTs.

Acknowledgments

We thank Mr John Martin for his linguistic assistance with the manuscript.

Funding Sources: This research did not receive any specific grant from funding agencies in the public, commercial, or not-for-profit sectors.

Disclosures: The authors have no conflicts to disclose.

Appendix

Supplementary Data

Supplementary data associated with this article can be found in the online version at https://doi.org/10.1016/j.hrcr.2023.09.013.

References

1. Kim YH, Chen SA, Ernst S, et al. 2019 APHRS expert consensus statement on three-dimensional mapping systems for tachycardia developed in collaboration with HRS, EHRA, and LAHRS. J Arrhythm 2020;36:215–270.
2. Hawson J, Anderson RD, Al-Kaisey A, et al. Functional assessment of ventricular tachycardia circuits and their underlying substrate using automated conduction velocity mapping. JACC Clin Electrophysiol 2022;8:480–494.
3. Ciaccio EJ, Anter E, Coromilas J, et al. Structure and function of the ventricular tachycardia isthmus. Heart Rhythm 2022;19:137–153.
4. Tung R, Raiman M, Liao H, et al. Simultaneous endocardial and epicardial delineation of 3D reentrant ventricular tachycardia. J Am Coll Cardiol 2020;75:884–897.
5. Nishimura T, Shatz N, Weiss P, et al. Identification of human ventricular tachycardia demarcated by fixed lines of conduction block in a 3-dimensional hyperboloid circuit. Circulation 2023. https://doi.org/10.1161/CIRCULATIONAHA.123.065525.
6. Iden L, Weinert R, Groschke S, Kuhnhardt K, Richardt G, Borlich M. First experience and validation of the extended early meets late (EEML) tool as part of the novel CARTO software HD COLORING. J Interv Card Electrophysiol 2021;60:279–285.
7. Takigawa M, Relan J, Kitamura T, et al. Impact of spacing and orientation on the scar threshold with a high-density grid catheter. Circ Arrhythm Electrophysiol 2019;12:e007158.
8. Deno DC, Bhaskaran A, Morgan DJ, et al. High-resolution, live, directional mapping. Heart Rhythm 2020;17:1621–1628.
9. Hadjis A, Frontera A, Limite LR, et al. Complete electroanatomic imaging of the diastolic pathway is associated with improved freedom from ventricular tachycardia recurrence. Circ Arrhythm Electrophysiol 2020;13:e008651.